JCI The Journal of Clinical Investigation

# Neisseria gonorrhoeae induces local secretion of IL-10 at the human cervix to promote colonization

Yiwei Dai, … , Daniel C. Stein, Wenxia Song

*J Clin Invest.* 2024. https://doi.org/10.1172/JCI183331.

Research In-Press Preview Infectious disease

## Graphical abstract

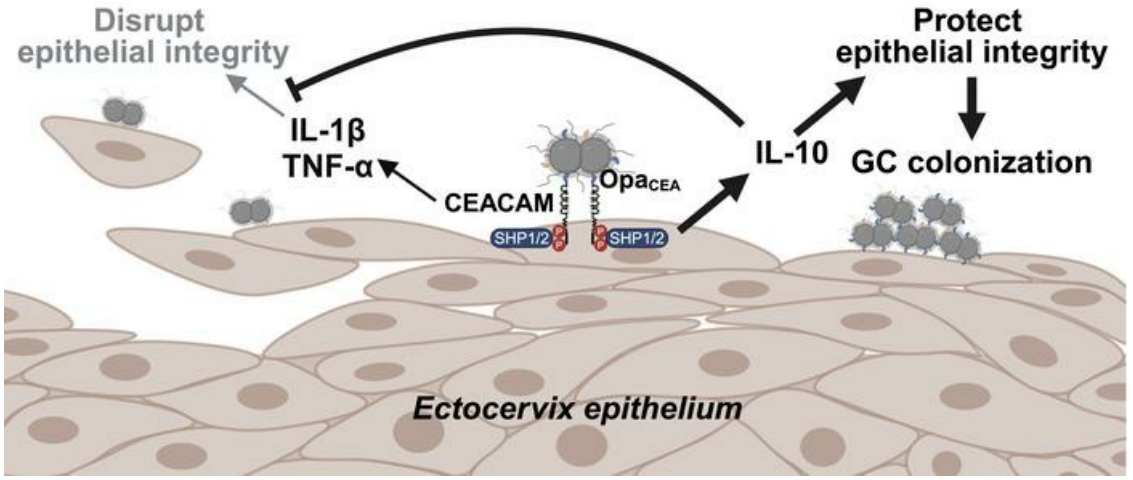

# *Neisseria gonorrhoeae induces local secretion of IL-10 at the human cervix to promote colonization*

*Yiwei Dai[1], Vonetta Edwards[2], Qian Yu[1], Hervé Tettelin[2], Daniel C. Stein[1], and Wenxia Song[1*]*

*[1]Department of Cell Biology and Molecular Genetics, University of Maryland, College Park, Maryland, USA*

*[2]Department of Microbiology and Immunology, Institute for Genome Sciences, University of Maryland School of Medicine, Baltimore, Maryland, USA*

*Qian Yu's current affiliation: Department of Internal Medicine, Yale University, New Haven, Connecticut, USA*

***Corresponding author:** Wenxia Song

Address: 2104 Bioscience Research Building, University of Maryland, College Park, MD 20742, USA

Phone number: 1-301-405-7552

Email: wenxsong@umd.edu

**Conflict-of-interest statement**

The authors have declared that no conflict of interest exists.

**Abstract**

Gonorrhea, caused by the human-restricted pathogen *Neisseria gonorrhoeae,* is a commonly reported sexually transmitted infection. Since most infections in women are asymptomatic, the true number of infections is likely much higher than reported. How gonococci (GC) colonize women's cervixes without triggering symptoms remains elusive. Using a human cervical tissue explant model, we found that GC inoculation increased the local secretion of both pro- (IL-1β and TNF-α) and anti-inflammatory (IL-10) cytokines during the first 24-h. Cytokine induction required GC expression of Opa isoforms that bind the host receptors carcinoembryonic antigen-related cell adhesion molecules (CEACAMs). GC inoculation induced NF-κB activation in both cervical epithelial and subepithelial cells. However, inhibition of NF-κB activation, which reduced GC-induced IL-1β and TNF-α, did not affect GC colonization. Neutralizing IL-10 or blocking IL-10 receptors by antibodies reduced GC colonization by increasing epithelial shedding and epithelial cell-cell junction disassembly. Inhibition of the CEACAM downstream signaling molecule SHP1/2, which reduced GC colonization and increased epithelial shedding, decreased GC-induced IL-10 secretion. These results show that GC induce local secretion of IL-10, a potent anti-inflammatory cytokine, at the cervix by engaging the host CEACAMs to prevent GC-colonizing epithelial cells from shedding, providing a potential mechanism for GC asymptomatic colonization in women.

## Introduction

Gonorrhea, caused by the Gram-negative bacterium *Neisseria gonorrhoeae,* is the second most common sexually transmitted infection (1). In women, most infections are asymptomatic or subclinical; therefore, the true number of infections is likely far higher than reported (2, 3). Gonococci (GC) infect humans exclusively, primarily targeting male and female urethras and the female cervix. GC can ascend from the vagina to the upper female reproductive tract (FRT) through the cervix, leading to severe clinical consequences, including pelvic inflammatory disease and infertility (4, 5). GC can colonize the lower part of the FRT asymptomatically for weeks and months (6, 7), allowing the bacteria to silently spread among sex partners and delaying the treatment until the infection permanently damages the FRT. Despite the clinical importance of asymptomatic infection, how GC colonize the human cervix without inducing symptoms or eliciting immune responses remains elusive. The primary obstacles in research of asymptomatic GC infection are the difficulties in clinically identifying and tracking asymptomatic carriers from the beginning of an infection and a lack of models that mimic asymptomatic infection in humans.

GC initiate infection at the FRT by colonizing the luminal epithelial cells of the cervix (8, 9) and can invade into epithelial cells (10, 11) and/or transmigrate across columnar epithelial cells (12, 13). GC use pili to initiate the interaction with epithelial cells, making it essential for GC colonization at the cervical epithelia (14-16). Mechanistically, pili retraction brings GC close to the luminal surface of epithelial cells (15, 17), allowing for the interaction of GC surface molecules, such as opacity-associated proteins (Opa), with their human-specific host receptors, such as carcinoembryonic antigen-related cell adhesion molecules (CEACAMs) and heparan

sulfate proteoglycans (HSPGs) (18, 19). We have previously established a human cervical tissue explant model and shown that this model recapitulates GC infection *in vivo* (16). GC preferentially colonize the ectocervix and transformation zone but selectively penetrate into the subepithelia of the transformation zone and endocervix of tissue explants, mimicking observations of patients' biopsies (8, 9, 16). Opas binding to CEACAMs ($Opa_{CEA}$) promote GC colonization and inhibit GC penetration at the human cervix by inhibiting GC-induced epithelial cell-cell junction disruption and epithelial shedding (13, 16, 20, 21). The inhibitory effects of $Opa_{CEA}$ on cervical colonization depend on the immunoreceptor tyrosine-based inhibitory motif (ITIM) in the cytoplasmic tails of CEACAM1 and its downstream signaling molecule SH2-containing protein tyrosine phosphatase (SHP) 1/2 (16). GC-induced epithelial cell shedding and the inhibitory effects of $Opa_{CEA}$ have also been observed in the cervix of vaginally infected mice that express human CEACAM5 and in human epithelial cell lines (20, 21). The fact that most of the 11 isoforms of Opa proteins bind to CEACAMs (22, 23) suggests that $Opa_{CEA}$-promoted colonization but not penetration enables GC survival on the human cervix.

The local cytokine response induced by microbial pathogens is one of the earliest warning signals for the immune system (24, 25). Inflammatory chemokines and cytokines can chemoattract and activate resident and circulating immune cells to clear the infection, with neutrophil infiltration being the main clinical feature of symptomatic GC infection (26). In contrast, a lack of a robust inflammatory cytokine response or an anti-inflammatory cytokine-dominated response can prohibit neutrophil infiltration (27). How GC escape or suppress local inflammatory responses to colonize women's cervix silently remains a critically unanswered question. The relationship between GC asymptomatic infection and the initial local cytokine

response of the cervix is unknown. Both inflammatory cytokines, such as IL-1β, TNF-α, and IL-17, and anti-inflammatory cytokines, such as IL-10 and TGF-β, have been detected in the cervical mucus of uninfected women (28-30). Elevation, reduction, and no change of both pro- and anti-inflammatory cytokines have all been reported previously in the cervical secretion of patients with GC infection, compared to uninfected controls (28, 31-34). This broad spectrum of data probably resulted from variations in sample collecting methods, sample collecting times relative to the menstrual cycle and GC infection course, and whether the infection was symptomatic or asymptomatic. *In vitro* studies have shown that GC induce the production of the anti-inflammatory cytokines IL-10 by human monocyte-derived dendritic cells (35), mouse bone marrow-derived dendritic cells (36), human monocyte-derived macrophages (37), human CD4+ T cells (38), human and mouse peripheral blood mononuclear cells (39, 40), mouse genital tract tissue explants (40), and cells from mouse iliac lymph nodes (40). As IL-10 is a master regulator of immunity and functions to protect hosts from over-exuberant responses (41-43), these data suggest inducing an anti-inflammatory cytokine response is a potential mechanism for GC to evade the host adaptive immunity when GC can enter tissues and directly interact with immune cells. However, the kind of cytokine responses colonizing GC can induce initially and locally at the human cervix and how induced cytokines impact immune detection are unknown.

In addition to activating inflammatory and anti-inflammatory responses, cytokines have been shown to regulate the barrier function and the homeostasis of the epithelium (44-46), potentially influencing the infection processes. The pro-inflammatory cytokines IL-1β and TNF-α, which are associated with inflammatory bowel diseases, disrupt epithelial cell-cell junctions by increasing the expression and activation levels of myosin light chain kinase (MLCK) (47-49).

TNF-α can also damage the epithelial barrier by inducing epithelial apoptosis, leading to shedding (50). In contrast, the anti-inflammatory cytokine IL-10 activates epithelial cell proliferation and wound repair, strengthening their barrier function (42, 43, 51, 52). The deficiency of IL-10 or IL-10 receptor (IL-10R) leads to human inflammatory bowel diseases (53, 54). However, the pleiotropic cytokine TGF-β can strengthen (such as in the intestine) (55) or weaken (such as in the uterus) (56) epithelial cell-cell junctions depending on its anatomic location. The cytokine environment of the human cervix and its role in GC infection have not been well studied.

This study examined the relationship between locally secreted cytokines and GC infection when the cervix is initially exposed to GC, using our human cervical tissue explant model. The explant model preserves the heterogeneous cervical epithelia and subepithelial cells and mimics *in vivo* GC infection with GC predominately colonizing the cervical epithelium (8, 9, 13, 16). Furthermore, it enables us to examine the earliest local cytokine response to GC colonization without the influence of blood and lymphoid circulation. This study focused on cytokines detected in female secretions and known to regulate epithelial integrity. Our results show that GC inoculation increases the secretion of the pro-inflammatory cytokines TNF-α and IL-1β by activating NF-κB and the secretion of the anti-inflammatory cytokine IL-10 by engaging the host receptor CEACAMs by Opa and activating CEACAM1 downstream signaling molecule SHP1/2. GC-induced pro-inflammatory cytokines TNF-α and IL-1β do not significantly affect GC colonization at the ectocervix. However, GC-induced anti-inflammatory cytokine IL-10 enhances GC colonization at the ectocervix by inhibiting GC-induced epithelial cell-cell junction disruption and the shedding of GC-associated cervical epithelial cells.

## Results

*GC inoculation increases the local secretion levels of both pro- and anti-inflammatory cytokines in the human cervix.* To determine the initial, local cytokine response of the cervix to GC infection, human cervical tissue explants (ecto- to endocervix) from the same donor were incubated without (No GC) or with MS11 GC strains with either all 11 isoforms of *opa* genes deleted (MS11ΔOpa) or the expression of a single non-phase variable $Opa_{52}$ protein that binds to CEACAMs ($MS11Opa_{CEA}$) at a MOI of 10 (10 bacteria per luminal epithelial cell) for 24 h at 37ºC. Since 10 of the 11 Opa isoforms in MS11 bind to CEACAMs (22, 23), $Opa_{52}$ was chosen to represent CEACAM-binding Opas. Culture supernatants were collected to quantify cytokine secretion using ELISA and Luminex Magpix. Cytokine levels were normalized to the luminal surface area of tissue explants and the volume of supernatant. Uninoculated tissue explants secreted detectable or modest amounts of pro-inflammatory cytokines IL-1β (Figure 1A) and TNF-α (Figure 1B), the anti-inflammatory cytokine IL-10 (Figure 1C), and the pleiotropic cytokine TGF-β (Figure 1D). Inoculation with $MS11Opa_{CEA}$, which colonize the cervical epithelium more efficiently than MS11ΔOpa (16), significantly increased both the pro- and anti-inflammatory cytokines but not TGF-β (Figure 1, A-D, and Table 1). However, inoculation with MS11ΔOpa GC, which colonize less but penetrate more efficiently than $MS11Opa_{CEA}$ (16), did not significantly elevate the level of these cytokines (Figure 1, A-D, and Table 1). IL-17A was undetectable in culture supernatants of GC uninoculated and inoculated cervical tissue explants (Figure 1E). When inoculating explants containing the ectocervix alone, the results were similar to those containing all three cervical regions (Figure 1, F-H, and Table 1). Inoculation with MS11ΔOpa GC slightly increased cytokines secreted by ectocervical tissue explants, like IL-1β and IL-10, but the increases were not statistically significant (Figure 1, F-H, and Table 1).

Because the two MS11Opa$_{CEA}$ and ΔOpa variants reached similar numbers after 24-h culture (Supplementary Figure 1), observed differences in cytokine responses cannot be due to growth differences. These data suggest that GC infection elevates the local secretion levels of both pro- and anti-inflammatory cytokines by the cervix during the first 24 h in an Opa$_{CEA}$-dependent manner.

*GC-induced pro-inflammatory cytokine secretion in the human cervix depends on NF-κB.* The transcription factor NF-κB is a crucial regulator of cytokine production (57, 58). To examine the possible involvement of NF-κB in GC-mediated cytokine expression, we determined if GC infection activated NF-κB in cervical cells using immunofluorescence microscopy. We measured the mean fluorescence intensity (MFI) of the NF-κB p65 subunit in the nuclei of individual cervical cells within the epithelium and subepithelium (135 μm below the epithelium) (Figure 2A and Supplementary Figure 2). MS11Opa$_{CEA}$ increased NF-κB p65 MFI in the nuclei of both epithelial and subepithelial cells of all three cervical regions, ectocervix (Ecto), transformation zone (TZ), and endocervix (Endo), compared to no GC controls (Figure 2B and Table 2). Among the three cervical regions of MS11Opa$_{CEA}$-infected tissue explants, the increases in the nuclear NF-κB p65 MFI of the ectocervical epithelial and subepithelial cells appeared to be higher than the other two cervical regions (Figure 2B and Table 2). However, MS11ΔOpa did not significantly change the NF-κB p65 MFI of the cervical epithelial cell nuclei (Figure 2B, left panel and Table 2). Interestingly, MS11ΔOpa reduced the nuclear NF-κB p65 MFI of subepithelial cells in the two GC-penetrated cervical regions, while slightly increasing the nuclear NF-κB p65 MFI of ectocervical subepithelial cells where MS11ΔOpa cannot penetrate (Figure 2B, right panel, and Table 2). Furthermore, both strains significantly increased the

mRNA expression levels of the NF-κB genes *NFKB2* and *RELB* and genes encoding proteins that act upstream of NF-κB activation and downstream of TNF-α and IL-1β, *TRAF1* and *IRAK2*, as measured by whole tissue NanoString-based transcriptomic analysis (Figure 2C). MS11Opa$_{CEA}$ also significantly elevated the mRNA levels of *NFKB1*, *RELA*, and *TRAF3* (Figure 2C). These data indicate that MS11Opa$_{CEA}$ inoculation increases NF-κB activation levels of both cervical epithelial and subepithelial cells.

To determine if GC-induced NF-κB activation is involved in the cytokine induction, we utilized a membrane-permeable small molecule inhibitor of NF-κB, Bay11-7082, that inhibits IκBα phosphorylation (59). The inhibitor (3 μM) was included in the 24 h incubation of ectocervical tissue explants with MS11Opa$_{CEA}$. Inhibitor treatment significantly reduced the NF-κB p65 MFI in the nuclei of ectocervical epithelial and subepithelial cells, even though the treatment did not bring their nuclear NF-κB p65 MFI back to the no GC level (Figure 2D and Table 3). However, the NF-κB inhibitor did not significantly affect GC growth (Supplementary Figure 3). Notably, the inhibitor treatment significantly reduced the secretion levels of the inflammatory cytokines IL-1β and TNF-α in the ectocervix but did not have a significant impact on the ectocervical secretion of the anti-inflammatory cytokine IL-10 (Figure 2E and Table 4). These data suggest that GC-induced pro- but not anti-inflammatory cytokine secretion involves NF-κB.

*Reductions in pro-inflammatory cytokines by NF-κB inhibition do not impact GC colonization of the ectocervix.* Treatment with the pro-inflammatory cytokine IL-1β or TNF-α disrupts epithelial cell-cell junctions and induces epithelial cell apoptosis, in addition to activating inflammation (44, 47). We determined whether NF-κB inhibition, which reduced IL-1β and TNF-α production

(Figure 2E), affected GC infection. Ectocervical tissue explants inoculated with MS11Opa$_{CEA}$ in the absence or presence of the NF-κB inhibitory Bay11-7082 (3 μM) were stained for GC (antibodies), DNA (Hoechst), and F-actin (phalloidin) to mark each ectocervical cell (Figure 3A). We quantified GC colonization by measuring the percentage of luminal epithelial cells with attached GC (Figure 3A, left panel), reflecting the extent of the epithelium being infected and GC fluorescence intensity (FI) per $\mu m^2$ of the luminal surface (Figure 3A, right panel), reflecting the relative amount of GC colonizing the ectocervical epithelium. Treatment with the NF-κB inhibitor changed neither the percentage of luminal ectocervical epithelial cells associated with GC (Figure 3B, left panel) nor the GC FI per $\mu m^2$ of the luminal surface significantly (Figure 3B, right panel). The NF-κB inhibitor also did not significantly affect GC growth (Supplementary Figure 3). We further quantified ectocervical epithelial cell shedding by measuring the percentage of the epithelial thickness and the percentage of epithelial cell layers remaining using no GC controls as 100% (Figure 3C). NF-κB inhibitor treatment did not affect the thickness (Figure 3D, left panel) or the cell layer number (Figure 3D, right panel) of the ectocervical epithelium. Even though the secreting levels of IL-1β and TNF-α were elevated in the absence of the NF-κB inhibitor (Figure 1, A and B), MS11Opa$_{CEA}$ GC inoculation did not induce significant changes in epithelial thickness and cell layers (Figure 3D). Together, these data suggest that GC-induced pro-inflammatory cytokines do not interfere with GC colonization of the human cervix.

*The anti-inflammatory cytokine IL-10 promotes GC colonization by inhibiting epithelial cell shedding.* In contrast to the pro-inflammatory cytokines IL-1β and TNF-α, the anti-inflammatory cytokine IL-10 has been shown to strengthen the barrier and wound repair functions of the epithelium (44, 51, 52). We determined whether MS11Opa$_{CEA}$-induced IL-10 production

contributes to GC infection, using either an IL-10 or IL-10 receptor (IL-10R) α antibody to prevent secreted IL-10 from engaging IL-10R (60, 61). Ectocervical tissue explants were inoculated with MS11Opa$_{CEA}$ in the absence or presence of IL-10 (10 μg/ml) or IL-10Rα (5 μg/ml) antibodies for 24 h. Luminex Magpix and ELISA analysis found that the IL-10 antibody effectively reduced the IL-10 level but did not significantly affect the levels of the pro-inflammatory cytokines IL-1β and TNF-α in the supernatants of ectocervical tissue explants inoculated with MS11Opa$_{CEA}$ (Figure 4A). IL-10 and IL-10Rα antibodies did not directly affect GC viability (Supplementary Figure 4). Immunofluorescence microscopic analysis found that the IL-10Rα antibody concentrated primarily at the ectocervical epithelium but could also be detected in the subepithelium (Supplementary Figure 5). Importantly, both IL-10 and IL-10Rα antibodies significantly reduced the percentages of the luminal epithelial cells associated with GC (Figure 4, B and C) and the GC FI per μm$^2$ (Figure 4, B and D), indicating reductions in GC colonization. Increased disassociation of GC-attached epithelial cells from the ectocervix was clearly visible in immunofluorescence images of IL-10 or IL-10Rα antibody-treated tissue explants, compared to untreated tissue explants (Figure 4B and Supplementary Figure 6, arrowheads). We quantified epithelial cell shedding using CFM images. Treatment with IL-10 and IL-10Rα antibodies resulted in reduced epithelial thickness (Figure 4E) and cell layer number (Figure 4F), as compared to untreated MS11Opa$_{CEA}$-infected ectocervical tissue explants as controls, indicating increased epithelial cell shedding. Using CFM images, we explored if IL-10 neutralization or IL-10Rα blocking induced epithelial shedding by disrupting epithelial cell-cell junction. We measured the fluorescence intensity ratios (FIR) of the ectocervical epithelial cell-cell junctional protein E-cadherin (E-cad) at the cell-cell junction relative to the cytoplasm using FI line profiles that vertically cross the epithelial cell-cell contact surface (Figure 4G).

Treatment of IL-10 or IL-10Rα antibodies significantly reduced the junction to cytoplasm ratios of E-cad FI (Figure 4H). Our results suggest that MS11Opa$_{CEA}$-induced IL-10 promotes bacterial colonization by strengthening epithelial cell-cell junctions and preventing epithelial cell shedding.

*GC induce IL-10 production by engaging CEACAM1 and activating SHP1/2.* Our previous studies have shown that GC interaction with CEACAM1 via Opa$_{CEA}$ increases GC colonization at the ectocervix by inhibiting epithelial cell shedding. This increase depends on the ITIM motif within the cytoplasmic domain of CEACAM1 and subsequent activation of SHP1/2 (16). Since MS11Opa$_{CEA}$ but not MS11ΔOpa increase cervical secretion of IL-10, we questioned whether GC induce IL-10 production through CEACAM1. We treated ectocervical tissue explants with NSC-87877, a membrane-permeable small molecule inhibitor of SHP1/2 (62) that inhibits the effects of Opa$_{CEA}$ on GC colonization and cervical epithelial shedding (16). We collected the supernatants from explants inoculated without or with MS11Opa$_{CEA}$ in the absence or presence of NSC-87877 (20 μM) and determined the concentration of IL-10, IL-1β, TNF-α, and TGF-β using Luminex Magpix or ELISA. Treatment with the SHP1/2 inhibitor significantly reduced the secreted IL-10 level by MS11Opa$_{CEA}$-inoculated tissue explants compared to tissue explants without the inhibitor (Figure 5A and Table 5). However, treatment of the SHP1/2 inhibitor did not significantly affect the secretion levels of the pro-inflammatory cytokines IL-1β and TNF-α and the pleiotropic cytokine TGF-β (Figure 5, B-D, and Table 5). This result suggests that GC induce IL-10 production but not IL-1β and TNF-α through CEACAM1 and the downstream SHP1/2, and GC-induced IL-10 contributed to Opa$_{CEA}$-mediated colonization enhancement.

## Discussion

This study utilized human cervical tissue explants as an infection model to demonstrate that GC inoculation increases the secretion levels of both the pro-inflammatory cytokines IL-1β and TNF-α and the anti-inflammatory cytokines IL-10 but not TGF-β and IL-17A during the first 24 h. The locally secreted anti-inflammatory cytokine IL-10, but not inflammatory cytokines IL-1β and TNF-α, modulates GC infection at the human cervix during this period. GC increase the secretion of IL-1β and TNF-α, but not IL-10, by activating NF-κB in both cervical epithelial and subepithelial cells. GC elevate the secretion of IL-10 but not IL-1β and TNF-α by binding to CEACAMs and activating their downstream SHP1/2. GC-induced IL-10 enhances GC colonization by inhibiting epithelial cell-cell junction disassembly and GC-associated cervical epithelial cell shedding.

A major finding of this study is that during the first 24 h of infection, GC colonization elevates the local secretion of the anti-inflammatory cytokine IL-10 at the cervix. While IL-10 was previously detected in women's cervical mucus, its level was reported to be increased, decreased, or unchanged by GC infection (31, 33, 34). However, in these studies, how long women had been infected before sample collection and whether infected women were symptomatic or asymptomatic were unknown. GC has been shown to elevate IL-10 levels when cultured with human monocyte-derived dendritic cells (35) and macrophages (37), CD4+ T cells (38), and mononuclear cells (39) from human peripheral blood. However, during the initial stage of natural infection (<24 h after exposure), GC primarily colonize the ectocervical epithelium (16) and have little chance of encountering subepithelial immune cells. Since the human cervical tissue explants are surgically disconnected from the blood and lymphatic circulation, our data provide

the first evidence for GC-elevated mucosal secretion of IL-10 by human cervical cells. These data together demonstrate the robust ability of GC to induce the production of IL-10, a potent anti-inflammatory cytokine, by the local mucosal or central immunity, depending on the types of cells they encounter. Whether GC-enhanced local secretion of IL-10 is sufficient to suppress inflammation activation associated with symptomatic infection is unknown. A major limitation of the current cervical tissue explant model is that it does not allow us to determine if the local cytokine response induces or suppresses the infiltration of neutrophils from the blood circulation. However, based on the potent inflammation inhibitory function of IL-10 (27), GC-induced elevation of IL-10 secretion at the cervix during the first 24 h of infection would negatively regulate local inflammation activation, consequently reducing blood immune cell infiltration and facilitating GC colonization.

This study found that cervical tissue explants constitutively secreted IL-10 at levels relatively higher than the basal level of the inflammatory cytokines IL-1β and TNF-α. Even though tissue wounding caused by surgery, tissue handling, and initial antibiotic treatment could modulate cytokine production, the relatively high basal level of IL-10 suggests an anti-inflammatory cytokine environment of the human cervix. This environment is consistent with the physiological functions of the cervix, a gate between the vagina and the uterus, which requires the cervix to tolerate semen and microbiota. The FRT is known to upregulate IL-10 production during pregnancy, which is critical for the immune tolerance of fetuses (63, 64). Here, we found that GC can further enhance the local production of IL-10 in the cervix. Furthermore, IL-10 neutralization and receptor blocking drastically increased epithelial shedding, but reductions in inflammatory cytokines did not. These results further support the notion that the anti-

inflammatory cytokine environment of the cervix, particularly the locally secreted IL-10, may effectively suppress the epithelial disrupting function of IL-1β and TNF-α, even when GC elevate the levels of IL-1β and TNF-α. However, this hypothesis requires further investigation.

Our results suggest that locally secreted IL-10 can directly act on cervical epithelial cells to promote GC colonization by inhibiting the disassembly of epithelial cell-cell junctions and GC-associated epithelial cell shedding. There are several potential mechanisms by which IL-10 can promote GC colonization at the cervix: activating epithelial cell proliferation, differentiation programs and wound repair pathways by directly engaging IL-10R on epithelial cells (41, 43), inhibiting pro-inflammatory cytokine production, and interfering with inflammatory cytokine-induced signaling pathways (27, 41) and mediated functions, including epithelial junction disrupting function (45, 49, 65). Here, we show that IL-10 neutralization or IL-10Rα blocking by antibodies weakens the epithelial cell-cell junction but does not increase the secretion of IL-1β and TNF-α by the cervix, suggesting that the observed effect of IL-10 is not mediated through downregulating the secretion of inflammatory cytokines but via interfering with their epithelial junction disrupting function. However, locally secreted IL-10 may inhibit inflammatory cytokine production *in vivo*. The unchanged levels of inflammatory cytokines we observed could be due to the failure of IL-10 and IL-10Rα antibodies to reach inflammatory cytokine-producing cells in the subepithelium of the cervix. The primary location of IL-10Rα blocking antibody at the luminal layer of the ectocervical epithelium suggests that IL-10Rα antibody only blocked IL-10 from binding IL-10R at the luminal surface of cervical epithelial cells. IL-10-mediated inhibition of shedding GC-associated cervical epithelial cells in the presence of the potent inflammatory

cytokines IL-1β and TNF-α underscores the importance of the direct interaction of IL-10 with IL-10R on epithelial cells for GC-establishing infection at the human cervix.

The elevated levels of inflammatory cytokines and nuclear NF-κB, a crucial transcriptional factor that controls the production of inflammatory cytokines (57, 58), by GC inoculation, suggest that GC cannot escape immune detection. Instead, GC increase the secretion of anti-inflammatory cytokines to counteract inflammation activation and maintain or even enhance immune tolerance in the cervix, depending on the relative levels of pro- and anti-inflammatory cytokines. GC can activate cervical cell signaling, such as Toll-like receptor (TLR) and inflammasome pathways (66, 67), through surface molecules, including pili, LOS, and peptidoglycans (68-72), leading to NF-κB activation. Interestingly, MS11Opa$_{CEA}$, which primarily colonize the luminal surface of the cervical epithelial cells, activate NF-κB in both epithelial and subepithelial cells, suggesting the activation of NF-κB in subepithelial cells may be indirect, probably through inflammatory cytokines secreted by cervical epithelial cells. Surprisingly, MS11ΔOpa, which can penetrate into the subepithelium of the transformation zone and the endocervix and may directly interact with subepithelial immune cells, do not significantly elevate IL-1β, TNF-α, and IL-10 at the first 24-h window. The weak local cytokine response induced by MS11ΔOpa is associated with a lower level of increase in NF-κB in the nuclei of epithelial cells and even reductions in NF-κB in the nuclei of subepithelial cells. As MS11Opa$_{CEA}$ was generated by introducing an Opa$_{CEA}$ to MS11ΔOpa (73) and showed similar growth rates, our data suggest a requirement of the Opa-CEACAM interaction to induce IL-1β and TNF-α production. However, inhibition of CEACAM1 downstream SHP1/2 slightly but not significantly reduced MS11Opa$_{CEA}$-induced IL-1β and TNF-α, which argues against this notion.

Besides activating SHP1/2, Opa-CEACAM interactions enhance GC colonization efficiency at the cervix (16), increasing the number of GC that interact with epithelial cells directly, which potentially enables higher levels of TLR, inflammasome, and cervical cell signaling activation, leading to their downstream NF-κB activation and pro-inflammatory cytokine secretion. This multifaceted hypothesis remains to be tested. On the other hand, MS11ΔOpa-induced NF-κB reduction in the nuclei of the subepithelial cells suggests an Opa-independent mechanism for GC suppression of inflammatory responses.

This study suggests that GC elevate the IL-10-secreting levels in the human cervix by engaging CEACAM1, which contains an ITIM motif in the cytoplasmic tail and can activate SHP1/2 downstream. Our supporting data include the induction of IL-10 by MS11Opa$_{CEA}$ but not MS11ΔOpa and reductions of both IL-10 secretion and MS11Opa$_{CEA}$ cervical colonization (16) by the SHP1/2 inhibitor. Which types of cervical cells respond to CEACAM1 binding to secret IL-10 remains unknown. Immune cells are the primary sources of IL-10, but non-immune cells, such as epithelial cells, can also secrete IL-10 (43, 74). In addition to cervical epithelial cells (16), many types of immune cells express CEACAM1 (75), include T cells where it functions as a negative regulator (76-78). CEACAM1 knockout in mice leads to the hyper-expansion of conventional T cells but the reduction of regulatory T cells, IL-10 producers, in the liver (79). *In vitro* experiments have shown that GC inhibits T cell receptor (TCR)-mediated human T cell activation by engaging CEACAM1 on the T cell surface by Opa and activating CEACAM1-downstream SHP1/2, downregulating TCR signaling (80, 81). GC has also been shown *in vitro* to promote macrophage polarization towards an alternatively activated phenotype characterized by heightened IL-10 production (37). Accumulating evidence supports Opa-CEACAM1

interactions as one of the mechanisms for GC to induce IL-10 production. However, this does exclude other possible mechanisms for GC to regulate IL-10 production in the cervix.

Many human factors can influence the cytokine production of the cervix, such as donors' ethnic background, age, microbiome, hormonal cycle, and clinical history, which are likely the sources of our data variability. Microbiomes and female sex hormones have all been shown to regulate the mucosal immunity of the FRT (82, 83). This study is just the beginning of the exploration of the relationship between the local cytokine responses and GC infection. Our human cervical explant model and the results of this study provide a step forward to our future study on how human cervical microbiome and female sex hormones regulate the local cytokine response to GC infection.

Our study reveals a new mechanism GC employ to evade mucosal immunity for colonization, enhancing local secretion of the anti-inflammatory cytokine IL-10 at the mucosal surface of the cervix by engaging CEACAM1. IL-10 then directly acts on cervical epithelial cells, preventing GC-colonizing epithelial cells from shedding off, in addition to its immune-suppressing function. Our results lead to a new hypothesis that GC induce early and local IL-10 production in the cervix to promote asymptomatic infection in women. This hypothesis potentially explains why CEACAM-binding Opa proteins have been evolutionally favored (22, 23).

## Methods

*Sex as a biological variable.* Our study exclusively examined *Neisseria gonorrhoeae* infection of the human cervix. Cervical tissues from female donors were used. Human cervical tissues used were anonymized. No race or ethnic information was provided.

*Neisseria strains. N. gonorrhoeae* strain MS11 with all 11 *opa* gene deleted (ΔOpa) and MS11 ΔOpa expressing non-phase variable CEACAM-binding $Opa_{52}$ ($Opa_{CEA}$) (73) were used. Piliated bacteria were identified based on colony morphology using a dissecting light microscope. GC were grown on plates with GC media and 1% Kellogg's supplement (GCK) for 16–18 h before inoculation. The concentration of bacteria in suspension was determined by using a spectrophotometer.

*Bacterial growth rates.* MS11$Opa_{CEA}$ and ΔOpa were cultured in CMRL-1066 media containing 5% FBS for 0, 6, 12, and 24 h in the absence and presence of the NF-κB inhibitor Bay11-7082, DMSO, the IL-10 neutralization (10 μg/ml), or IL-10 receptor (IL-10R) α-blocking antibodies (5 μg/ml). Bacteria were enumerated by counting CFU after serially diluting tissue culture media and plating on GCK plates or quantified by optical density at 650 nm.

*Human cervical tissue explants.* Healthy cervical tissues were obtained from donors (28–42 years old) undergoing hysterectomies for medical reasons unrelated to the cervix and received within 24 h post-surgery through the National Disease Research Interchange (NDRI). In addition to the donors' age, a pathology report of the cervix came with each tissue shipment. Only cervical tissues without pathological changes were used. Tissue explants were generated and

processed using a previously published protocol (84). Briefly, Muscle parts of the tissue were removed using a carbon steel surgical blade. Cervical tissues from one human subject were cut into three or four equal pieces with the dimension of ~2.5 cm (L) X 0.6 cm (W) X 0.3 cm (H) for comparing different inoculation conditions. For ectocervix tissue explants, ectocervical tissues were separated from the transformational zone and endocervix by visual inspection. Tissue explants were incubated in the CMRL-1066 (11530037, Gibco), containing 5% heat-inactivated fetal bovine serum (A5256701, Gibco), L-glutamine (2 mM, 25030081, Gibco), bovine insulin (1 μg/ml, 16634, Sigma-Aldrich), and penicillin/streptomycin for 24 h, followed by antibiotic-free media for another 24 h. GC were inoculated at MOI ~10 (10 bacteria to 1 luminal epithelial cell). The number of epithelial cells at the luminal surface was determined by the luminal surface area of individual explants divided by the average luminal area of individual cervical epithelial cells (25 $\mu m^2$). The cervical tissue explants were incubated with GC at 37°C with 5% $CO_2$ with gentle shaking for 24 h and washed with antibiotic-free cervical tissue culture medium at 6 and 12 h to remove non-adhered bacteria.

*Inhibitor and antibody treatment.* Cervical tissue explants were incubated with bacteria in the presence or absence of NF-κB inhibitor BAY 11-7082 (3 μM, HY-13453, MedChemExpress) (59), SHP inhibitor NSC-87877 (85) (20 μM, 565851-50MG, EMD Millipore), rat anti-human IL-10 antibody (10 μg/ml, 10100-01, SouthernBiotech), or rat anti-human IL-10Rα antibody (5 μg/ml, 308802, BioLegend) for 24 h. The inhibitors and the antibodies were replenished after the 6 and 12 h washing.

*Quantification of Cytokine secretion.* Supernatants collected from cervical tissue explants at 6, 12, and 24 h post-inoculation were pooled together in an 1:1:2 volume ratio, and a protease inhibitor cocktail (PIC0002, Sigma-Aldrich) was added to prevent protein degradation. Supernatants collected from cervical tissue explants used for previous studies on GC infectivity and infection mechanism (16) were utilized for cytokine quantification for Figures 1, A-E, and 5. Cytokines in the supernatants were quantified using a Luminex Magpix system (Bio-Plex® MAGPIX™ Multiplex Reader, Bio-Rad Laboratories) and the Human XL Cytokine Luminex Performance Assay 46-Plex Fixed Panel (Bio-Techne), according to the manufacturer's protocol. The secretion levels of IL-1β and TGF-β were quantified using enzyme-linked immunosorbent assay (ELISA) by human IL-1β ELISA Max Deluxe kit (437004, BioLegend) and human TGF-β1 duoset ELISA kit (Dy204-05, R&D System). Each sample was run in duplicate. The cytokine concentrations of each sample by either Luminex Magpix or ELISA were normalized based on the supernatant volume and the tissue luminal surface area.

*Immunofluorescence analysis of human cervical tissue explants.* The tissue explants were fixed in 4% paraformaldehyde 24 h post-inoculation, embedded in 20% gelatin, cryopreserved, sectioned crossing the luminal, basal surfaces of the epithelium and subepithelial tissues, stained for F-actin (100 nM, phalloidin, PHDH1, Cytoskeleton), E-cadherin (mouse anti-human E-cadherin antibody, 5 µg/ml, 610182, BD Bioscience), NF-κB p65 (rabbit anti-human p65 antibody, 5 µg/ml, 8242, Cell Signaling Technology), and GC (custom polyclonal antibody) (84) by specific antibodies, and nuclei by Hoechst (20 µg/ml, H3570, Life Technologies), and imaged using confocal fluorescence microscope (CFM, Zeiss LSM 980, Carl Zeiss Microscopy LLC). Images were acquired using Zeiss Zen software.

The levels of NF-κB activation were quantified by the mean fluorescence intensity (MFI) of p65 staining in individual nuclei. Individual nucleus was identified by Hoechst staining using NIH ImageJ. The data were generated using 3-4 human cervixes, 2 independent analyses per cervix, 5-11 randomly acquired images per ectocervical region, 3-8 randomly acquired images per TZ region, 3-10 randomly acquired images per endocervical region per analysis, including 200 nuclei per ectocervical epithelial region, 70 nuclei per ectocervical subepithelial region, 35 nuclei per transformation zone epithelial region, 45 nuclei per transformation zone subepithelial region, 35 nuclei per endocervical epithelial region, and 170 nuclei per endocervical subepithelial region per analysis.

The levels of GC colonization at the ectocervix were quantified by two methods using CFM images (16): (1) the percentage of luminal epithelial cells with GC attached at the luminal surface by manually accounting and (2) the fluorescence intensity (FI) of GC staining per $\mu m^2$ of the luminal surface using the NIH ImageJ software. The data were generated from 2-4 human cervixes, 3 independent analyses per cervix, and 3-10 randomly acquired images per analysis.

The levels of epithelial shedding in the ectocervix were determined by two methods (16): (1) the percentage of the remaining thickness (μm) of the epithelium and (2) the percentage of remaining epithelial cell layers (based on F-actin staining) compared to uninfected ectocervical tissue explants, using the NIH ImageJ software. The data were generated from 2-4 human cervixes, 3 independent analyses per cervix, and 3-10 randomly acquired images per analysis.

The redistribution of E-cadherin from the cell-cell junction to the cytoplasm was evaluated by the fluorescence intensity ratios (FIR) of E-cadherin staining at the cell-cell junction relative to the cytoplasm in individual epithelial cells using CFM images by the NIH ImageJ software. The data were generated from 2-4 human cervixes, 3 independent analyses per cervix, and 4-10 randomly acquired images per analysis.

*Gene expression analysis by NanoString.* At 24 h post-inoculation, the tissue explants were embedded in Tissue-Tek® O.C.T. Compound (4583, Sakura Finetek) and snap froze in liquid nitrogen. Thirty 10-μm thickness tissue sections were collected from each tissue explant for RNA isolation using RNeasy Mini Kit (74104, Qiagen). The multiplexed NanoString nCounter™ Immunology Panel (PSTD Hs Immunology V2-12, NanoString Technologies) with 594 genes was used, according to the manufacturer's protocol. The data QC, background threshold, normalization, and differential gene expression analysis were conducted using nSolver™ Analysis software. The quality of the run for each sample was confirmed by the quality control, including the 6 spiked-in RNA positive controls and the 8 negative controls present in the panel, the FOV (fields of view per sample) counted, and the binding density. Gene expression data were normalized by using the 15 housekeeping genes present in the panels. Background level was determined by mean counts of 8 negative control probes plus two standard deviations. When a gene's raw counts are below the background of >50% of all samples, this gene is excluded from differential expression analysis. Differential gene expression analysis was performed by comparing the normalized count of each gene in infected samples and uninfected samples, and genes with $p < 0.05$ were identified as differential expression genes.

*Statistical analysis.* Statistical significance was assessed using the Student's *t*-test and ANOVA by Prism software (GraphPad). A P value less than 0.05 was considered significant.

*Study approval.* Human cervical tissues were obtained through the National Disease Research Interchange (NDRI, Philadelphia, PA). Human cervical tissues used were anonymized. No race or ethnic information was provided. The use of human tissues has been approved by the Institution Review Board of the University of Maryland.

*Data availability.* The Supporting Data Values file is provided in the supplementary materials.

**Acknowledgments**

We thank the UMD CBMG Imaging Core for all microscopy experiments and the Maryland Genomics Core at the University of Maryland School of Medicine for the NanoString transcriptomic analysis. This work was supported by a grant (AI141894) from the National Institutes of Health to DCS and WS.

**Author contributions**

WS conceptualized the study. YD, VE, and QY performed experiments and analyzed data. HT analyzed transcriptomic data. DCS generated genetically modified bacterial strains. WS and YD wrote the manuscript. DCS, HT, and VE reviewed and edited the manuscript. All authors approved the final version of the manuscript.

## References


1. CDC. Sexually transmitted infection surveillance 2022.
2. Elder H, Platt L, Leach D, Sheetoh C, Ramirez VM, Molotnikov L, et al. Factors associated with delays in presentation and treatment of gonorrhea, Massachusetts 2015-2019. *Sex Transm Dis.* 2024;51(3):146-55.
3. Detels R, Green AM, Klausner JD, Katzenstein D, Gaydos C, Handsfield H, et al. The incidence and correlates of symptomatic and asymptomatic Chlamydia trachomatis and *Neisseria gonorrhoeae* infections in selected populations in five countries. *Sex Transm Dis.* 2011;38(6):503-9.
4. Darville T. Pelvic inflammatory disease due to *Neisseria gonorrhoeae* and *Chlamydia trachomatis*: Immune evasion mechanisms and pathogenic disease pathways. *J Infect Dis.* 2021;224(12 Suppl 2):S39-S46.
5. Xu SX, and Gray-Owen SD. Gonococcal pelvic inflammatory disease: Placing mechanistic insights into the context of clinical and epidemiological observations. *J Infect Dis.* 2021;224(12 Suppl 2):S56-S63.
6. Stupiansky NW, Van Der Pol B, Williams JA, Weaver B, Taylor SE, and Fortenberry JD. The natural history of incident gonococcal infection in adolescent women. *Sex Transm Dis.* 2011;38(8):750-4.
7. Lovett A, and Duncan JA. Human immune responses and the natural history of *Neisseria gonorrhoeae* infection. *Front Immunol.* 2018;9:3187.
8. Evans BA. Ultrastructural study of cervical gonorrhea. *J Infect Dis.* 1977;136(2):248-55.
9. Harkness AH. The pathology of gonorrhoea. *Br J Vener Dis.* 1948;24(4):137-47.

10. McGee ZA, Stephens DS, Hoffman LH, Schlech WF, and Horn RG. Mechanisms of mucosal invasion by pathogenic *Neisseria*. *Rev Infect Dis.* 1983;5 Suppl 4:S708-14.

11. Dehio C, Gray-Owen SD, and Meyer TF. Host cell invasion by pathogenic *Neisseriae*. *Subcell Biochem.* 2000;33:61-96.

12. Merz AJ, Rifenbery DB, Arvidson CG, and So M. Traversal of a polarized epithelium by pathogenic *Neisseriae*: facilitation by type IV pili and maintenance of epithelial barrier function. *Mol Med.* 1996;2(6):745-54.

13. Wang LC, Yu Q, Edwards V, Lin B, Qiu J, Turner JR, et al. *Neisseria gonorrhoeae* infects the human endocervix by activating non-muscle myosin II-mediated epithelial exfoliation. *PLoS Pathog.* 2017;13(4):e1006269.

14. Stephens DS, Krebs JW, and McGee ZA. Loss of pili and decreased attachment to human cells by *Neisseria meningitidis* and *Neisseria gonorrhoeae* exposed to subinhibitory concentrations of antibiotics. *Infect Immun.* 1984;46(2):507-13.

15. Hockenberry AM, Hutchens DM, Agellon A, and So M. Attenuation of the type IV pilus retraction motor influences *Neisseria gonorrhoeae* social and infection behavior. *mBio.* 2016;7(6).

16. Yu Q, Wang LC, Di Benigno S, Gray-Owen SD, Stein DC, and Song W. *Neisseria gonorrhoeae* infects the heterogeneous epithelia of the human cervix using distinct mechanisms. *PLoS Pathog.* 2019;15(12):e1008136.

17. Merz AJ, So M, and Sheetz MP. Pilus retraction powers bacterial twitching motility. *Nature.* 2000;407(6800):98-102.

18. Sintsova A, Wong H, MacDonald KS, Kaul R, Virji M, and Gray-Owen SD. Selection for a CEACAM receptor-specific binding phenotype during *Neisseria gonorrhoeae* infection of the human genital tract. *Infect Immun.* 2015;83(4):1372-83.

19. Chen T, Belland RJ, Wilson J, and Swanson J. Adherence of pilus- Opa+ gonococci to epithelial cells in vitro involves heparan sulfate. *J Exp Med.* 1995;182(2):511-7.

20. Muenzner P, Rohde M, Kneitz S, and Hauck CR. CEACAM engagement by human pathogens enhances cell adhesion and counteracts bacteria-induced detachment of epithelial cells. *J Cell Biol.* 2005;170(5):825-36.

21. Muenzner P, Bachmann V, Zimmermann W, Hentschel J, and Hauck CR. Human-restricted bacterial pathogens block shedding of epithelial cells by stimulating integrin activation. *Science.* 2010;329(5996):1197-201.

22. Bos MP, Grunert F, and Belland RJ. Differential recognition of members of the carcinoembryonic antigen family by Opa variants of *Neisseria gonorrhoeae*. *Infect Immun.* 1997;65(6):2353-61.

23. Gray-Owen SD, Lorenzen DR, Haude A, Meyer TF, and Dehio C. Differential Opa specificities for CD66 receptors influence tissue interactions and cellular response to *Neisseria gonorrhoeae*. *Mol Microbiol.* 1997;26(5):971-80.

24. Bamias G, Arseneau KO, and Cominelli F. Cytokines and mucosal immunity. *Curr Opin Gastroenterol.* 2014;30(6):547-52.

25. Mettelman RC, Allen EK, and Thomas PG. Mucosal immune responses to infection and vaccination in the respiratory tract. *Immunity.* 2022;55(5):749-80.

26. Stevens JS, and Criss AK. Pathogenesis of *Neisseria gonorrhoeae* in the female reproductive tract: neutrophilic host response, sustained infection, and clinical sequelae. *Curr Opin Hematol.* 2018;25(1):13-21.

27. Couper KN, Blount DG, and Riley EM. IL-10: the master regulator of immunity to infection. *J Immunol.* 2008;180(9):5771-7.

28. Masson L, Salkinder AL, Olivier AJ, McKinnon LR, Gamieldien H, Mlisana K, et al. Relationship between female genital tract infections, mucosal interleukin-17 production and local T helper type 17 cells. *Immunology.* 2015;146(4):557-67.

29. Tanko RF, Bunjun R, Dabee S, Jaumdally SZ, Onono M, Nair G, et al. The effect of contraception on genital cytokines in women randomized to copper intrauterine device, depot medroxyprogesterone acetate, or levonorgestrel implant. *J Infect Dis.* 2022;226(5):907-19.

30. Sharma P, Shahabi K, Spitzer R, Farrugia M, Kaul R, and Yudin M. Cervico-vaginal inflammatory cytokine alterations after intrauterine contraceptive device insertion: A pilot study. *PLoS One.* 2018;13(12):e0207266.

31. Hedges SR, Sibley DA, Mayo MS, Hook EW, and Russell MW. Cytokine and antibody responses in women infected with *Neisseria gonorrhoeae*: effects of concomitant infections. *J Infect Dis.* 1998;178(3):742-51.

32. Geisler WM, Wang C, Tang J, Wilson CM, Crowley-Nowick PA, and Kaslow RA. Immunogenetic correlates of *Neisseria gonorrhoeae* infection in adolescents. *Sex Transm Dis.* 2008;35(7):656-61.

33. Maina A, Mureithi M, Kiiru J, and Revathi G. Systemic and mucosal concentrations of nine cytokines among individuals with *Neisseria gonorrhoeae* infection in Nairobi Kenya. *AAS Open Res.* 2022;5:12.

34. Cohen CR, Plummer FA, Mugo N, Maclean I, Shen C, Bukusi EA, et al. Increased interleukin-10 in the the endocervical secretions of women with non-ulcerative sexually transmitted diseases: a mechanism for enhanced HIV-1 transmission? *AIDS.* 1999;13(3):327-32.

35. van Vliet SJ, Steeghs L, Bruijns SC, Vaezirad MM, Snijders Blok C, Arenas Busto JA, et al. Variation of *Neisseria gonorrhoeae* lipooligosaccharide directs dendritic cell-induced T helper responses. *PLoS Pathog.* 2009;5(10):e1000625.

36. Zhu W, Ventevogel MS, Knilans KJ, Anderson JE, Oldach LM, McKinnon KP, et al. *Neisseria gonorrhoeae* suppresses dendritic cell-induced, antigen-dependent CD4 T cell proliferation. *PLoS One.* 2012;7(7):e41260.

37. Ortiz MC, Lefimil C, Rodas PI, Vernal R, Lopez M, Acuña-Castillo C, et al. *Neisseria gonorrhoeae* modulates immunity by polarizing human macrophages to a M2 profile. *PLoS One.* 2015;10(6):e0130713.

38. Plant LJ, and Jonsson AB. Type IV pili of *Neisseria gonorrhoeae* influence the activation of human CD4+ T cells. *Infect Immun.* 2006;74(1):442-8.

39. Rarick M, McPheeters C, Bright S, Navis A, Skefos J, Sebastiani P, et al. Evidence for cross-regulated cytokine response in human peripheral blood mononuclear cells exposed to whole gonococcal bacteria in vitro. *Microb Pathog.* 2006;40(6):261-70.

40. Liu Y, Liu W, and Russell MW. Suppression of host adaptive immune responses by *Neisseria gonorrhoeae*: role of interleukin 10 and type 1 regulatory T cells. *Mucosal Immunol.* 2014;7(1):165-76.

41. Saraiva M, Vieira P, and O'Garra A. Biology and therapeutic potential of interleukin-10. *J Exp Med.* 2020;217(1).

42. Shouval DS, Ouahed J, Biswas A, Goettel JA, Horwitz BH, Klein C, et al. Interleukin 10 receptor signaling: master regulator of intestinal mucosal homeostasis in mice and humans. *Adv Immunol.* 2014;122:177-210.

43. Nguyen HD, Aljamaei HM, and Stadnyk AW. The production and function of endogenous Interleukin-10 in intestinal epithelial cells and gut homeostasis. *Cell Mol Gastroenterol Hepatol.* 2021;12(4):1343-52.

44. Al-Sadi R, Boivin M, and Ma T. Mechanism of cytokine modulation of epithelial tight junction barrier. *Front Biosci (Landmark Ed).* 2009;14(7):2765-78.

45. Andrews C, McLean MH, and Durum SK. Cytokine Tuning of Intestinal Epithelial Function. *Front Immunol.* 2018;9:1270.

46. Capaldo CT, and Nusrat A. Cytokine regulation of tight junctions. *Biochim Biophys Acta.* 2009;1788(4):864-71.

47. Kaminsky LW, Al-Sadi R, and Ma TY. IL-1β and the intestinal epithelial tight junction barrier. *Front Immunol.* 2021;12:767456.

48. Al-Sadi R, Ye D, Dokladny K, and Ma TY. Mechanism of IL-1beta-induced increase in intestinal epithelial tight junction permeability. *J Immunol.* 2008;180(8):5653-61.

49. Al-Sadi R, Guo S, Ye D, and Ma TY. TNF-α modulation of intestinal epithelial tight junction barrier is regulated by ERK1/2 activation of Elk-1. *Am J Pathol.* 2013;183(6):1871-84.

50. Grabinger T, Bode KJ, Demgenski J, Seitz C, Delgado ME, Kostadinova F, et al. Inhibitor of apoptosis protein-1 regulates tumor necrosis factor-mediated destruction of intestinal epithelial cells. *Gastroenterology.* 2017;152(4):867-79.

51. Jarry A, Bossard C, Bou-Hanna C, Masson D, Espaze E, Denis MG, et al. Mucosal IL-10 and TGF-beta play crucial roles in preventing LPS-driven, IFN-gamma-mediated epithelial damage in human colon explants. *J Clin Invest.* 2008;118(3):1132-42.

52. Morhardt TL, Hayashi A, Ochi T, Quirós M, Kitamoto S, Nagao-Kitamoto H, et al. IL-10 produced by macrophages regulates epithelial integrity in the small intestine. *Sci Rep.* 2019;9(1):1223.

53. Madsen KL, Malfair D, Gray D, Doyle JS, Jewell LD, and Fedorak RN. Interleukin-10 gene-deficient mice develop a primary intestinal permeability defect in response to enteric microflora. *Inflamm Bowel Dis.* 1999;5(4):262-70.

54. Glocker EO, Kotlarz D, Boztug K, Gertz EM, Schäffer AA, Noyan F, et al. Inflammatory bowel disease and mutations affecting the interleukin-10 receptor. *N Engl J Med.* 2009;361(21):2033-45.

55. Howe KL, Reardon C, Wang A, Nazli A, and McKay DM. Transforming growth factor-beta regulation of epithelial tight junction proteins enhances barrier function and blocks enterohemorrhagic Escherichia coli O157:H7-induced increased permeability. *Am J Pathol.* 2005;167(6):1587-97.

56. Grant-Tschudy KS, and Wira CR. Paracrine mediators of mouse uterine epithelial cell transepithelial resistance in culture. *J Reprod Immunol.* 2005;67(1-2):1-12.

57. Pasparakis M. Role of NF-κB in epithelial biology. *Immunol Rev.* 2012;246(1):346-58.

58. Oeckinghaus A, and Ghosh S. The NF-kappaB family of transcription factors and its regulation. *Cold Spring Harb Perspect Biol.* 2009;1(4):a000034.

59. Strickson S, Campbell DG, Emmerich CH, Knebel A, Plater L, Ritorto MS, et al. The anti-inflammatory drug BAY 11-7082 suppresses the MyD88-dependent signalling network by targeting the ubiquitin system. *Biochem J.* 2013;451(3):427-37.

60. Kessler B, Rinchai D, Kewcharoenwong C, Nithichanon A, Biggart R, Hawrylowicz CM, et al. Interleukin 10 inhibits pro-inflammatory cytokine responses and killing of Burkholderia pseudomallei. *Sci Rep.* 2017;7:42791.

61. Tang X, Zhang S, Peng Q, Ling L, Shi H, Liu Y, et al. Sustained IFN-I stimulation impairs MAIT cell responses to bacteria by inducing IL-10 during chronic HIV-1 infection. *Sci Adv.* 2020;6(8):eaaz0374.

62. Chen L, Sung SS, Yip ML, Lawrence HR, Ren Y, Guida WC, et al. Discovery of a novel shp2 protein tyrosine phosphatase inhibitor. *Mol Pharmacol.* 2006;70(2):562-70.

63. Cheng SB, and Sharma S. Interleukin-10: a pleiotropic regulator in pregnancy. *Am J Reprod Immunol.* 2015;73(6):487-500.

64. Chatterjee P, Chiasson VL, Bounds KR, and Mitchell BM. Regulation of the anti-inflammatory cytokines Interleukin-4 and Interleukin-10 during pregnancy. *Front Immunol.* 2014;5:253.

65. Al-Sadi R, Guo S, Ye D, Dokladny K, Alhmoud T, Ereifej L, et al. Mechanism of IL-1β modulation of intestinal epithelial barrier involves p38 kinase and activating transcription factor-2 activation. *J Immunol.* 2013;190(12):6596-606.

66. Trinchieri G, and Sher A. Cooperation of Toll-like receptor signals in innate immune defence. *Nat Rev Immunol.* 2007;7(3):179-90.

67. Le J, Kulatheepan Y, and Jeyaseelan S. Role of toll-like receptors and nod-like receptors in acute lung infection. *Front Immunol.* 2023;14:1249098.

68. Meyer TF. Pathogenic *Neisseria*--interplay between pro- and eukaryotic worlds. *Folia Microbiol (Praha).* 1998;43(3):311-9.

69. Patrone JB, and Stein DC. Effect of gonococcal lipooligosaccharide variation on human monocytic cytokine profile. *BMC Microbiol.* 2007;7:7.

70. Liu M, John CM, and Jarvis GA. Phosphoryl moieties of lipid A from *Neisseria meningitidis* and *N. gonorrhoeae* lipooligosaccharides play an important role in activation of both MyD88- and TRIF-dependent TLR4-MD-2 signaling pathways. *J Immunol.* 2010;185(11):6974-84.

71. Knilans KJ, Hackett KT, Anderson JE, Weng C, Dillard JP, and Duncan JA. *Neisseria gonorrhoeae* lytic transglycosylases LtgA and LtgD reduce host innate immune signaling through TLR2 and NOD2. *ACS Infect Dis.* 2017;3(9):624-33.

72. Howie HL, Glogauer M, and So M. The *N. gonorrhoeae* type IV pilus stimulates mechanosensitive pathways and cytoprotection through a pilT-dependent mechanism. *PLoS Biol.* 2005;3(4):e100.

73. LeVan A, Zimmerman LI, Mahle AC, Swanson KV, DeShong P, Park J, et al. Construction and characterization of a derivative of *Neisseria gonorrhoeae* strain MS11 devoid of all *opa* genes. *J Bacteriol.* 2012;194(23):6468-78.

74. Saraiva M, and O'Garra A. The regulation of IL-10 production by immune cells. *Nat Rev Immunol.* 2010;10(3):170-81.

75. Gray-Owen SD, and Blumberg RS. CEACAM1: contact-dependent control of immunity. *Nat Rev Immunol.* 2006;6(6):433-46.

76. Nagaishi T, Pao L, Lin SH, Iijima H, Kaser A, Qiao SW, et al. SHP1 phosphatase-dependent T cell inhibition by CEACAM1 adhesion molecule isoforms. *Immunity.* 2006;25(5):769-81.

77. Chen Z, Chen L, Qiao SW, Nagaishi T, and Blumberg RS. Carcinoembryonic antigen-related cell adhesion molecule 1 inhibits proximal TCR signaling by targeting ZAP-70. *J Immunol.* 2008;180(9):6085-93.

78. Nagaishi T, Chen Z, Chen L, Iijima H, Nakajima A, and Blumberg RS. CEACAM1 and the regulation of mucosal inflammation. *Mucosal Immunol.* 2008;1 Suppl 1(0 1):S39-42.

79. Horst AK, Wegscheid C, Schaefers C, Schiller B, Neumann K, Lunemann S, et al. Carcinoembryonic antigen-related cell adhesion molecule 1 controls IL-2-dependent regulatory T-cell induction in immune-mediated hepatitis in mice. *Hepatology.* 2018;68(1):200-14.

80. Boulton IC, and Gray-Owen SD. Neisserial binding to CEACAM1 arrests the activation and proliferation of CD4+ T lymphocytes. *Nat Immunol.* 2002;3(3):229-36.

81. Lee HS, Ostrowski MA, and Gray-Owen SD. CEACAM1 dynamics during *Neisseria gonorrhoeae* suppression of CD4+ T lymphocyte activation. *J Immunol.* 2008;180(10):6827-35.

82. Brotman RM, Ravel J, Bavoil PM, Gravitt PE, and Ghanem KG. Microbiome, sex hormones, and immune responses in the reproductive tract: challenges for vaccine development against sexually transmitted infections. *Vaccine.* 2014;32(14):1543-52.

83. Wira CR, Rodriguez-Garcia M, and Patel MV. The role of sex hormones in immune protection of the female reproductive tract. *Nat Rev Immunol.* 2015;15(4):217-30.

84. Wang LC, Yu Q, Stein DC, and Song W. Immunofluorescence analysis of human endocervical tissue explants infected with *Neisseria gonorrhoeae*. *Bio Protoc.* 2018;8(3).

85. Song M, Park JE, Park SG, Lee DH, Choi HK, Park BC, et al. NSC-87877, inhibitor of SHP-1/2 PTPs, inhibits dual-specificity phosphatase 26 (DUSP26). *Biochem Biophys Res Commun.* 2009;381(4):491-5.

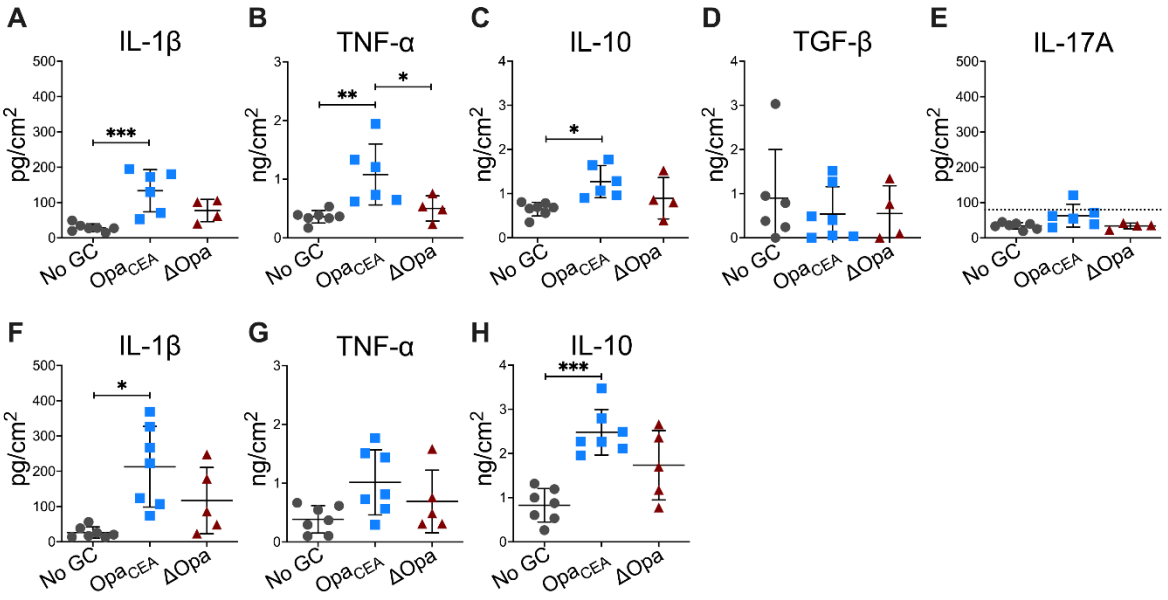


**Figure 1. GC inoculation increases the secretion of both pro- and anti-inflammatory cytokines by human cervical tissue explants.** Human cervical tissue explants with the ecto- to endocervix (**A-E**) or with the ectocervix alone (**F-H**) were incubated without (No GC) or with MS11 GC strains expressing no *opa* genes (ΔOpa) or a non-phase variable $Opa_{52}$ that binds to CEACAMs ($Opa_{CEA}$) at a MOI of 10 for 24 h at 37°C. Supernatants of cervical tissue explant media were collected. The average concentrations (±SD) of IL-1β (**A, F**), TNF-α (**B, G**), IL-10 (**C, H**), TGF-β (**D**), and IL-17A (**E**, dashed line, detection level) were measured by Luminex Magpix (IL-1β, TNF-α, IL-10, and IL-17A) or ELISA (TGF-β), normalized to the luminal surface areas of tissue explants and supernatant volumes. Data points represent cervical tissues from individual human subjects. The data were generated from 3-7 cervixes. * $p<0.05$, ** $p<0.01$, *** $p<0.001$, by One-Way ANOVA.

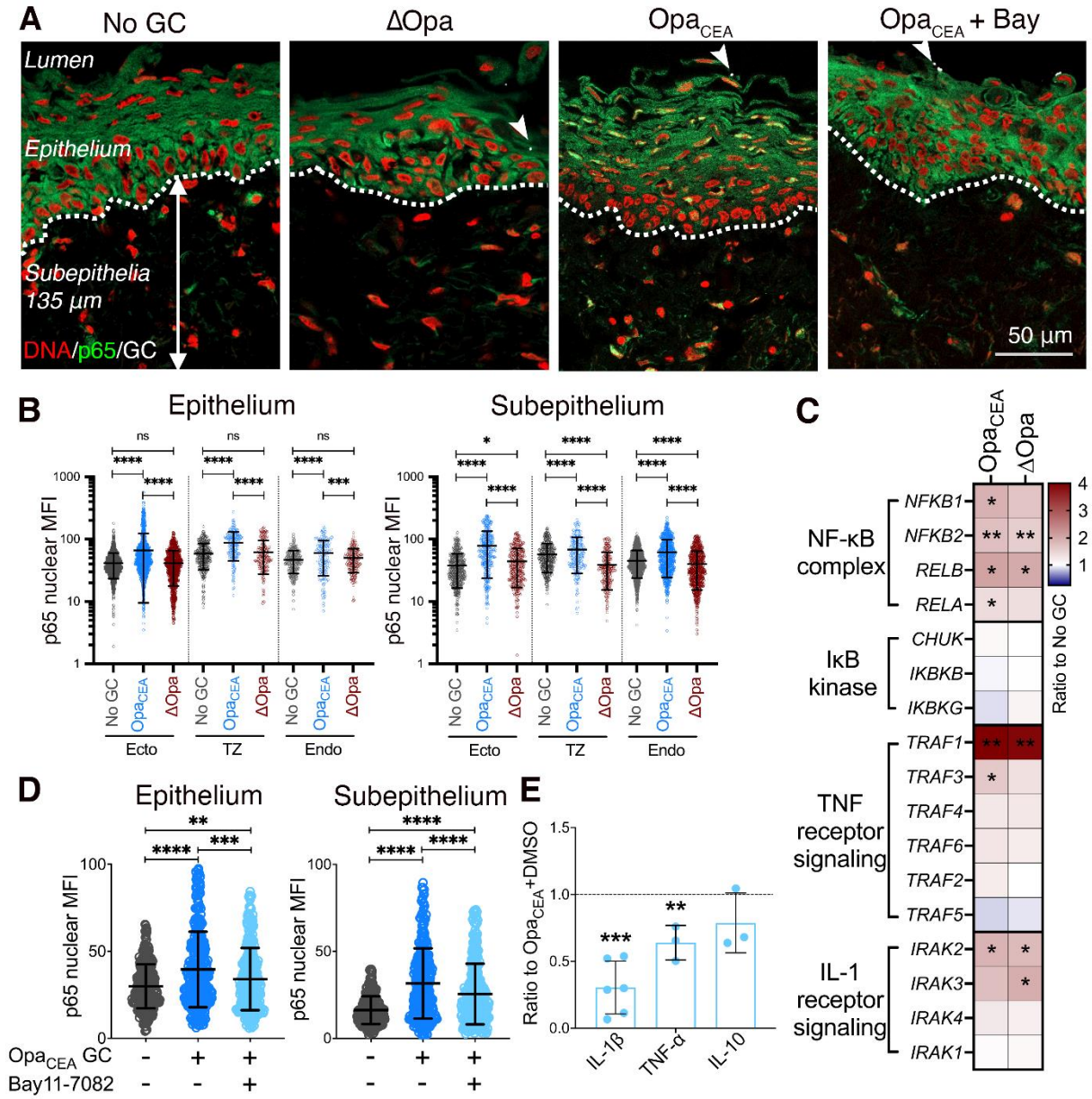


**Figure 2. NF-κB is involved in GC-induced pro-inflammatory cytokine production by the human cervix.** Human cervical tissue explants were incubated without or with MS11Opa$_{CEA}$ or MS11ΔOpa (MOI~10) in the absence or presence of the NF-κB inhibitor Bay11-7082 (3 µM) for 24 h. The culture supernatants were collected, and tissues were cryopreserved. (**A**) Tissue sections were stained for NF-κB p65 and GC by antibodies and nuclei by Hoechst and imaged

using a confocal fluorescence microscope (CFM). Representative images of the ectocervix without or with MS11Opa$_{CEA}$ or ΔOpa GC inoculation in the absence or presence of the NF-κB inhibitor Bay11-7082 are shown. White dashed lines outline the epithelium, arrows indicate the 135 μm depth of the subepithelium, and arrowheads point to GC attached to the epithelium. Scale bar, 50 μm. (**B**) The mean fluorescent intensity (MFI) (±SD) of NF-κB p65 in the nuclei of individual epithelial and subepithelial cells (135 μm below the epithelium) in the ectocervix (Ecto), transformation zone (TZ), and endocervix (Endo) were measured. Data points represent individual nuclei. Data were generated from cervical tissues from 3-4 human subjects, 2 independent analyses per cervix, and 35-200 epithelial and 45-170 subepithelial cells per analysis per cervical region. (**C**) A heatmap shows the relative mRNA levels of NF-κB-related genes determined by the NanoString Immunology panel. RNAs were isolated from cervical tissue explants inoculated without (no GC) or with MS11Opa$_{CEA}$ or ΔOpa GC. The comparisons of MS11Opa$_{CEA}$- or ΔOpa-inoculated with no GC control tissues from 3 human subjects are shown. (**D**) The nuclear MFI of NF-κB p65 in individual epithelial and subepithelial cells from the ectocervical tissue explants inoculated without or with MS11Opa$_{CEA}$ in the absence or presence of Bay11-7082. Datapoint represents individual nuclei. The average values (±SD) were generated from ectocervical tissues from 3 human subjects, 3 independent analyses per cervix, and 40 nuclei per region per analysis. (**E**) The concentrations of IL-1β, TNF-α, and IL-10 in the supernatants of ectocervical tissue explants inoculated with MS11Opa$_{CEA}$ in the absence and presence of Bay11-7082 were measured using Luminex Magpix (IL-1β, TNF-α and IL-10) and ELISA (IL-1β) and normalized to the luminal surface areas and the supernatant volume of individual explants. Shown are the ratios of cytokine concentrations (±SD) secreted by ectocervical tissue explants inoculated with MS11Opa$_{CEA}$ in the presence of Bay11-7082

compared to those MS11Opa$_{CEA}$ inoculated in the presence of the vehicle control DMSO. Data points represent individual analysis. * $p$<0.05, ** $p$<0.01, *** $p$<0.001, **** $p$<0.0001, by One-Way ANOVA (**B**-**D**) and unpaired student's $t$-test (**E**).

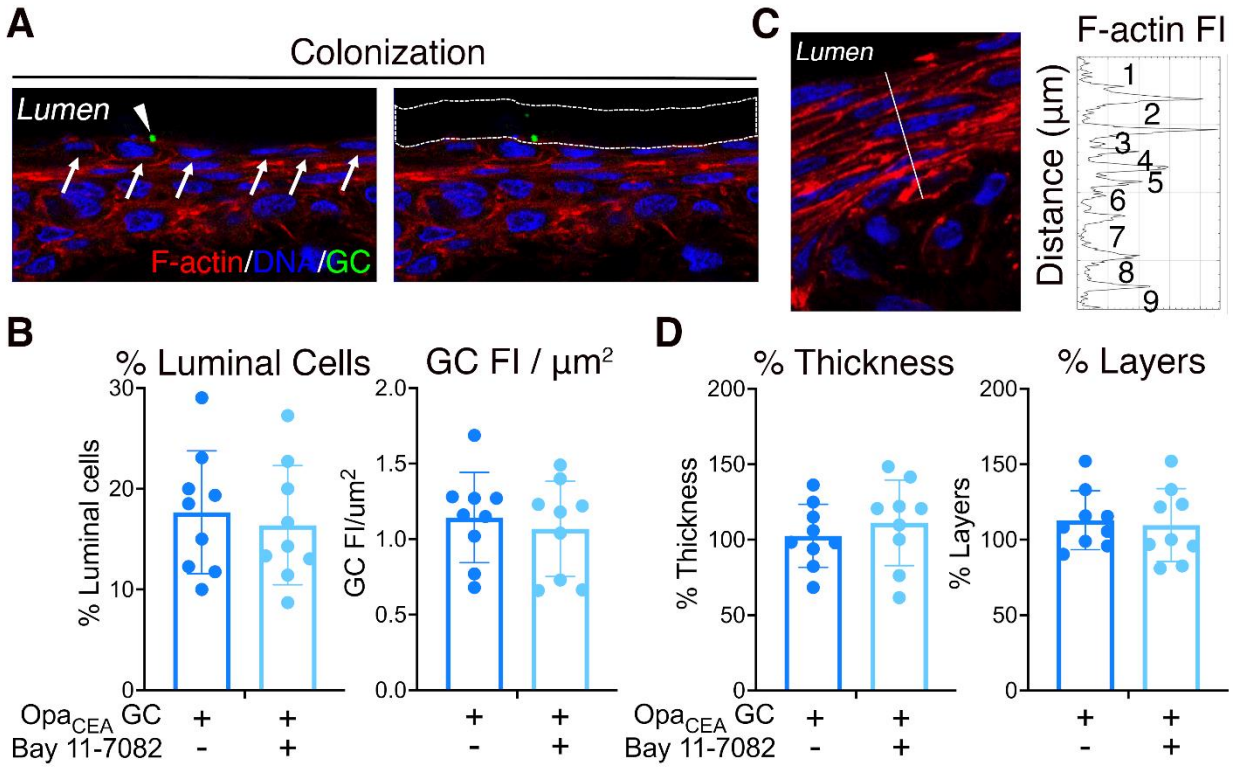


**Figure 3. Pro-inflammatory cytokine reduction by NF-κB inhibition does not affect GC colonization of the ectocervix and ectocervical epithelial shedding.** Human ectocervical tissue explants were inoculated without or with MS11Opa$_{CEA}$ in the absence and presence of the NF-κB inhibitor Bay11-7082 (3 µM) for 24 h (MOI~10) and cryopreserved. Tissue sections were stained for GC by a polyclonal antibody, DNA by Hoechst, and F-actin by phalloidin and analyzed using CFM. (**A**) Quantification of GC colonization by the percentage of luminal epithelial cells associated with GC (left panel) and by fluorescence intensity (FI) of GC staining per µm$^2$ of the luminal surface (right panel). Arrows in the left panel point to individual luminal epithelial cells and arrowhead to a GC-associated luminal epithelial cell. White dashed lines in the right panel outline the luminal surface area where GC FI was measured. (**B**) The average percentages (±SD) of luminal epithelial cells associated with GC and the average value of GC FI per µm$^2$ of the luminal surface from ectocervical tissues of 3 human subjects with 3 independent

analyses per cervix and 3-10 randomly acquired images per analysis. Data points represent each independent analysis. (**C**) Quantification of epithelium shedding by the percentage of remaining epithelium thickness (left panel, the length of the dashed line vertical against the epithelium) and cell layers based on the FI line profile of F-actin staining on the dashed line (right panel), compared with no GC control. (**D**) The average percentages (±SD) of the remaining epithelial thickness (Left panel) and cell layers (Right panel) from ectocervical tissues of 3 human subjects with 3 independent analyses per cervix, 3-10 randomly acquired images per analysis, and 3 line profiles per image. Data points represent each independent analysis. There are no significant differences by unpaired student's *t*-test.

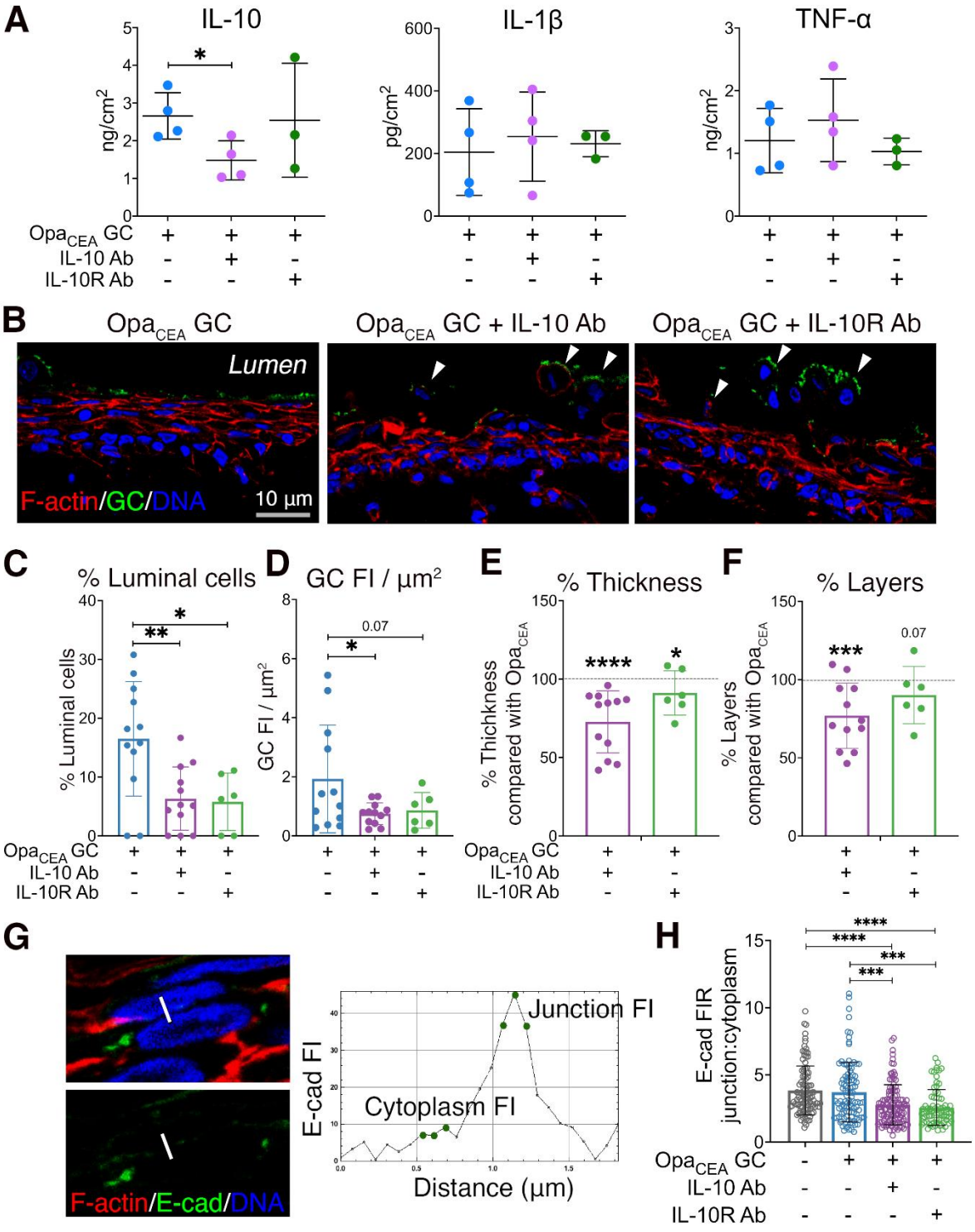
A
IL-10
IL-1β
TNF-α
ng/cm2
pg/cm2
ng/cm2
*
OpaCEA GC
IL-10 Ab
IL-10R Ab
B
OpaCEA GC
OpaCEA GC + IL-10 Ab
OpaCEA GC + IL-10R Ab
Lumen
F-actin/GC/DNA
10 μm
C
% Luminal cells
% Luminal cells
D
GC FI / μm2
GC FI / μm2
0.07
E
% Thickness
% Thickness compared with OpaCEA
****
F
% Layers
% Layers compared with OpaCEA
***
0.07
G
F-actin/E-cad/DNA
E-cad FI
Junction FI
Cytoplasm FI
Distance (μm)
H
E-cad FIR junction:cytoplasm
****
***

**Figure 4. IL-10 neutralization and IL-10 receptor-blocking antibodies reduce GC colonization by increasing ectocervical epithelial cell shedding.** Human ectocervical tissue explants were incubated without and with MS11Opa$_{CEA}$ in the absence and presence of anti-IL-10 (10 μg/ml) or IL-10Rα antibody (5 μg/ml) for 24 h (MOI~10). The culture supernatants were collected, and tissues were cryopreserved. (**A**) The concentrations of IL-10, IL-1β, and TNF-α in the supernatants were measured by Luminex Magpix. Data points represent individual cervixes. n=3-4. (**B)** Representative images of ectocervical tissue sections stained for GC, DNA, and F-actin. Arrowhead, shed epithelial cells. Scale bar, 10 μm. (**C** and **D**) Quantification of GC colonization by the percentage (±SD) of luminal epithelial cells associated with GC (**C**) and by FI (±SD) of GC staining per μm$^2$ of the luminal surface (**D**). Shown are the average values from 2-4 cervixes, 3 independent analyses per cervixes, and 4-8 randomly acquired images per analysis. Data points represent independent analysis. (**E** and **F**) Quantification of epithelium shedding by the percentages (±SD) of remaining epithelium thickness (**E**) and cell layers (**F**) in tissue explants inoculated with MS11Opa$_{CEA}$ in the presence of IL-10 or IL-10Rα antibody, compared to tissue explants inoculated with MS11Opa$_{CEA}$ without IL-10 or IL-10Rα antibody. Shown are the average values from 2-4 cervixes and 3 independent analyses per cervix. Data points represent independent analysis. (**G** and **H**) Disruption of epithelial cell-cell junctions was determined by the FI ratio (FIR) of E-cad at the cell-cell border relative to the cytoplasm (**H)** using the average FI of three data points (green dots) along line profiles (**G).** Shown are the average FIR (±SD) from 2-4 cervixes with 3 independent analyses per cervix, 4-10 randomly acquired images per analysis, and 3 line profiles per image. Data points represent individual line profiles. ** $p<0.01$, *** $p<0.001$, **** $p<0.001$, by One-Way ANOVA.

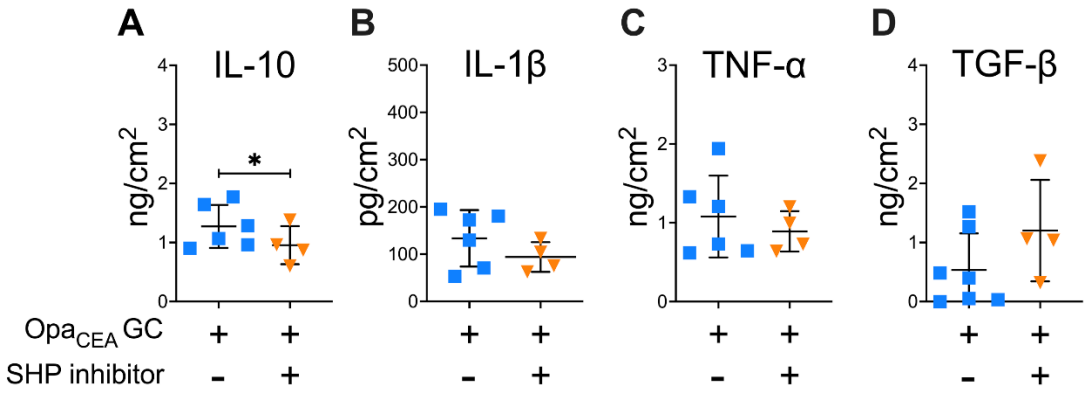


**Figure 5. GC-induced IL-10 but not IL-1β and TNF-α secretion by human cervical tissue explants requires CEACAM1 signaling.** Supernatants of cervical tissue explants inoculated with MS11Opa$_{CEA}$ in the absence or presence of the SHP1/2 inhibitor NSC-87877 (20 μM) for 24 h were collected. The cytokine concentrations were measured by Luminex Magpix or ELISA (TGF-β) and normalized to the luminal surface area and the supernatant volume of each explant. Shown are the average concentration (±SD) from 4-7 cervixes. Data points represent individual cervixes. * $p$<0.05, ** $p$<0.01, *** $p$<0.001 by unpaired student's $t$-test.

**Table 1. Cytokine secretion levels by GC inoculated human cervical tissue explants.**

| | | Mean | SD | p-value to No GC | p-value to $Opa_{CEA}$ |
|---|---|---|---|---|---|
| **Ecto- to endocervix** | | | | | |
| **IL-1β** (pg/cm$^2$) | | | | | |
| | No GC | 28.76 | 11.09 | | |
| | $Opa_{CEA}$ | 133.55 | 59.78 | 0.0008 | |
| | ΔOpa | 77.53 | 31.61 | 0.1537 | 0.1042 |
| **TNF-α** (ng/cm$^2$) | | | | | |
| | No GC | 0.36 | 0.11 | | |
| | $Opa_{CEA}$ | 1.08 | 0.52 | 0.0044 | |
| | ΔOpa | 0.5 | 0.21 | 0.7787 | 0.0438 |
| **IL-10** (ng/cm$^2$) | | | | | |
| | No GC | 0.65 | 0.16 | | |
| | $Opa_{CEA}$ | 1.27 | 0.36 | 0.0115 | |
| | ΔOpa | 0.9 | 0.47 | 0.5723 | 0.2523 |
| **TGF-β** (ng/cm$^2$) | | | | | |
| | No GC | 0.9 | 1.1 | | |
| | $Opa_{CEA}$ | 0.54 | 0.62 | | |
| | ΔOpa | 0.55 | 0.63 | | |
| **IL-17A** (pg/cm$^2$) | | | | | |
| | No GC | 34.24 | 9.13 | | |
| | $Opa_{CEA}$ | 63.04 | 32.35 | 0.0603 | |
| | ΔOpa | 33.97 | 8.10 | 0.9998 | 0.1082 |
| **Ectocervix** | | | | | |
| **IL-1β** (pg/cm$^2$) | | | | | |
| | No GC | 26.33 | 15.90 | | |
| | $Opa_{CEA}$ | 212.88 | 114.51 | 0.0292 | |
| | ΔOpa | 116.98 | 93.98 | 0.3081 | 0.2961 |
| **TNF-α** (ng/cm$^2$) | | | | | |
| | No GC | 0.38 | 0.23 | | |
| | $Opa_{CEA}$ | 1.01 | 0.55 | 0.0435 | |
| | ΔOpa | 0.69 | 0.53 | 0.3925 | 0.4800 |
| **IL-10** (ng/cm$^2$) | | | | | |
| | No GC | 0.83 | 0.38 | | |
| | $Opa_{CEA}$ | 2.48 | 0.51 | 0.0010 | |
| | ΔOpa | 1.73 | 0.79 | 0.2148 | 0.3915 |

The data were generated from 4-7 cervixes and analyzed by One-Way ANOVA. See details in Figure 1.

**Table 2. NF-κB p65 MFI in the nuclei of individual epithelial and subepithelial cells in the ectocervix, transformation zone, and endocervix.**

| | Mean | SD | p-value to No GC | p-value to $Opa_{CEA}$ |
|---|---|---|---|---|
| **Epithelium** | | | | |
| **Ecto** | | | | |
| No GC | 41.68 | 18.38 | | |
| $Opa_{CEA}$ | 66.49 | 56.99 | <0.0001 | |
| ΔOpa | 41.44 | 23.67 | 0.9839 | <0.0001 |
| **TZ** | | | | |
| No GC | 59.15 | 26.92 | | |
| $Opa_{CEA}$ | 87.96 | 43.05 | <0.0001 | |
| ΔOpa | 61.72 | 34.24 | 0.6976 | <0.0001 |
| **Endo** | | | | |
| No GC | 47.03 | 18.85 | | |
| $Opa_{CEA}$ | 60.17 | 34.29 | <0.0001 | |
| ΔOpa | 49.95 | 21.01 | 0.409 | 0.0005 |
| **Subepithelium** | | | | |
| **Ecto** | | | | |
| No GC | 37.81 | 21.35 | | |
| $Opa_{CEA}$ | 79.08 | 55.54 | <0.0001 | |
| ΔOpa | 44.31 | 27.43 | 0.0231 | <0.0001 |
| **TZ** | | | | |
| No GC | 57.11 | 28.07 | | |
| $Opa_{CEA}$ | 68.11 | 39.78 | <0.0001 | |
| ΔOpa | 38.6 | 23.26 | <0.0001 | <0.0001 |
| **Endo** | | | | |
| No GC | 45.03 | 21.12 | | |
| $Opa_{CEA}$ | 61.51 | 37.25 | <0.0001 | |
| ΔOpa | 40.06 | 24.78 | <0.0001 | <0.0001 |

Data were generated from 3-4 cervixes, 2 independent analyses per cervix, and 35-200 epithelial and 45-170 subepithelial cells per analysis per cervical region and analyzed by One-Way ANOVA. See details in Figure 2B.

**Table 3. NF-κB p65 MFI in the nuclei of individual epithelial and subepithelial cells in ectocervical tissue explants inoculated without or with MS11Opa$_{CEA}$ in the absence or presence of Bay11-7082.**

| | Mean | SD | p-value to No GC | p-value to Opa$_{CEA}$ GC |
|---|---|---|---|---|
| **Epithelium** | | | | |
| No GC | 31.10 | 14.55 | | |
| Opa$_{CEA}$+DMSO | 41.27 | 23.84 | <0.0001 | |
| Opa$_{CEA}$+Bay | 34.77 | 18.85 | 0.0078 | 0.0002 |
| **Subepithelium** | | | | |
| No GC | 16.80 | 8.83 | | |
| Opa$_{CEA}$+DMSO | 31.98 | 20.74 | <0.0001 | |
| Opa$_{CEA}$+Bay | 25.78 | 17.80 | <0.0001 | <0.0001 |

Data were generated from 3 cervixes, 3 independent analyses per cervix, and 40 nuclei per region per analysis and analyzed by One-Way ANOVA. See details in Figure 2D.

**Table 4. Treatment of an NF-κB inhibitor, Bay11-7082, reduces the production of IL-1β and TNF-α in the cervix induced by MS11Opa$_{CEA}$.**

| | Mean | SD | p-value |
|---|---|---|---|
| **GC+Bay to GC+DMSO Ratio** | | | |
| IL-1β | 0.3 | 0.2 | 0.0006 |
| TNF-α | 0.64 | 0.13 | 0.0085 |
| IL-10 | 0.79 | 0.22 | 0.1755 |

Data were generated from 3 cervixes, 2 independent analyses per cervix for IL-1β, and analyzed by unpaired student's t-test. See details in Figure 2E.

**Table 5. Levels of cytokine secretion by GC inoculated human cervical tissue explants treated without or with the SHP inhibitor.**

| | Mean | SD | p-value to $Opa_{CEA}$ |
|---|---|---|---|
| **IL-10** (ng/cm$^2$) | | | |
| $Opa_{CEA}$ | 1.27 | 0.36 | |
| $Opa_{CEA}$ + SHP inhibitor | 0.96 | 0.32 | 0.0423 |
| **IL-1β** (pg/cm$^2$) | | | |
| $Opa_{CEA}$ | 133.55 | 59.78 | |
| $Opa_{CEA}$ + SHP inhibitor | 93.93 | 31.48 | 0.4269 |
| **TNF-α** (ng/cm$^2$) | | | |
| $Opa_{CEA}$ | 1.08 | 0.52 | |
| $Opa_{CEA}$ + SHP inhibitor | 0.89 | 0.26 | 0.3994 |
| **TGF-β** (ng/cm$^2$) | | | |
| $Opa_{CEA}$ | 0.54 | 0.62 | |
| $Opa_{CEA}$ + SHP inhibitor | 1.2 | 0.86 | 0.3156 |

The data were generated from 4-7 cervixes and analyzed by unpaired student's *t*-test. See details in Figure 5.